

# On the angle between the first and the second Lyapunov vectors in spatio-temporal chaos

D Pazó, J M López and M A Rodríguez

Instituto de Física de Cantabria (IFCA), CSIC-Universidad de Cantabria,  
E-39005 Santander, Spain

**Abstract.** In a dynamical system the first Lyapunov vector (LV) is associated with the largest Lyapunov exponent and indicates —at some point on the attractor— the direction of maximal growth in tangent space. The LV corresponding to the second largest Lyapunov exponent generally points at a different direction, but tangencies between both vectors can in principle occur. Here we find that the probability density function (PDF) of the angle  $\psi$  spanned by the first and the second LVs should be expected approximately symmetric around  $\pi/4$  and peaked at 0 and  $\pi/2$ . Moreover, for small angles we uncover a scaling law for the PDF  $Q$  of  $\psi_l = \ln \psi$  with the system size  $L$ :  $Q(\psi_l) = L^{-1/2} f(\psi_l L^{-1/2})$ . We give a theoretical argument that justifies this scaling form and also explains why it should be universal (irrespective of the system details) for spatio-temporal chaos in one spatial dimension.

PACS numbers: 05.45Jn, 05.45Ra, 05.10.Gg

## 1. Introduction

The Lyapunov exponents are fundamental quantifiers of chaos (Ott 1993). The directions in phase space associated with them are generally referred to as the Lyapunov vectors (LVs). It is clear that the Lyapunov vectors should play an important role, at least conceptually, in predictability questions in meteorology (Kalnay 2002) and related sciences, or in achieving a microscopic description of many particle systems (Taniguchi & Morriss 2005).

Since 2007 (Wolfe & Samelson 2007, Szendro et al. 2007, Ginelli et al. 2007), there has been a growing awareness in the scientific community that the set of vectors obtained as a byproduct of the standard method to compute the Lyapunov exponents (Benettin et al. 1980) is not the most suitable way of defining the Lyapunov vectors due to a series of artefacts these vectors exhibit. The so-called characteristic (or covariant) Lyapunov vectors (CLVs) are known since long time ago (Eckmann & Ruelle 1985) to be the only intrinsic (metric-independent) basis of LVs, but only since 2007 their computation has become more or less routine. The use of these vectors has been probably more abundant in the field of meteorology due to their implication in predictability questions (Legras & Vautard 1996, Trevisan & Pancotti 1998, Pazó et al. 2010, Ng et al. 2011, Herrera et al. 2011).

CLVs define the so-called Oseledec splitting or decomposition of tangent space. The concept of dominated decomposition is used in the mathematical literature and basically implies that the Oseledec subspaces are dynamically isolated. This is

supposed not to be generically the case in extended systems with spatio-temporal chaos (Yang & Radons 2008, Yang et al. 2009). However there is a lack of theoretical tools allowing to know in advance how the angles between subspaces should be distributed. Questions concerning the angles between the CLVs and the subspaces they span have been addressed numerically in the context of hydrodynamical Lyapunov modes (Yang & Radons 2008, Bosetti & Posch 2010, Morriss & Truant 2012), inertial manifolds (Yang et al. 2009), and hyperbolicity (Kuptsov & Parlitz 2010). In sum there is a growing interest on the angles among CLVs in spatially extended chaotic systems, which reflects in the latest publications on this subject (Morriss 2012).

The seminal work by Pikovsky & Politi (1998) demonstrated that in extensive chaos, the first LV exhibits universal scaling laws in space and time falling into universality class of the KPZ equation (Kardar et al. 1986). Some system-independent scaling laws have been much more recently detected for LVs corresponding to LEs smaller than the largest one (Szendro et al. 2007, Pazó et al. 2008). This justifies the expectation that the angle between the LVs should obey as well some universal features at a scaling level. Eventually, the final picture of the relations between different CLVs should be consistent with the extensive nature of spatio-temporal chaos (Ruelle 1979, Cross & Hohenberg 1993).

In this work we demonstrate that the probability density function (PDF) of the angle between the two leading CLVs has universal features. For small angle values, we uncover a universal (i.e. system-independent) scaling law with the system size. Our theoretical arguments make use of (i) the formulas intrinsic to the method by Wolfe & Samelson (2007), and (ii) the belonging (under a suitable transformation) of the first LV to the universality class of the KPZ equation.

## 2. Lyapunov vectors: Definitions

In a  $N$ -dimensional dynamical system infinitesimal perturbations  $\delta\mathbf{u}$  evolve governed by linear equations (the so-called ‘linear tangent model’). This implies the existence of a linear operator  $\mathbf{M}$  that transforms the perturbation at a given time  $t_1$  into the perturbation at another time  $t_0$ :

$$\delta\mathbf{u}(t_0) = \mathbf{M}(t_0, t_1)\delta\mathbf{u}(t_1) \quad (1)$$

with the obvious properties  $\mathbf{M}(t_0, t_0) = \mathbb{I}$  and  $\mathbf{M}(t_1, t_0) = \mathbf{M}^{-1}(t_0, t_1)$ .

### 2.1. Backward Lyapunov vectors

The multiplicative ergodic theorem (Oseledec 1968) (see e.g., (Eckmann & Ruelle 1985)) establishes the existence of a limit operator

$$\Phi_b(t_0) = \lim_{t_1 \rightarrow -\infty} [\mathbf{M}(t_0, t_1)\mathbf{M}^*(t_0, t_1)]^{\frac{1}{2(t_0 - t_1)}} \quad (2)$$

where the asterisk denotes the adjoint operator, such that the logarithms of the eigenvalues of  $\Phi_b$  are the LEs  $\{\lambda_n\}_{n=1, \dots, N}$ . By convention we assume  $\lambda_n \geq \lambda_{n+1}$ . Note that, in contrast to the LEs, the operator  $\Phi_b$  depends on the position in the attractor (parametrized by  $t_0$ ). Moreover the metric determining the adjoint of  $\mathbf{M}$  is relevant (although irrelevant concerning the LEs). Thus the eigenvectors of  $\Phi_b$  form an orthonormal basis  $\{\mathbf{b}_n(t_0)\}_{n=1, \dots, N}$ , within the particular metric adopted. This set of eigenvectors, so-called *backward* LVs (Legras & Vautard 1996), serve to define a set of nested subspaces. The first LV  $\mathbf{b}_1(t_0)$  generates the straight line  $S_1(\mathbf{x}_0)$  corresponding

to infinitesimal perturbations at  $\mathbf{x}_0 = \mathbf{x}(t_0)$  that shrink as  $\sim \exp(\lambda_1 t)$  as  $t \rightarrow -\infty$ .  $\mathbf{b}_1(t_0)$  and  $\mathbf{b}_2(t_0)$  define the plane  $S_2(\mathbf{x}_0)$ , such that the modulus of infinitesimal perturbations initially inside  $S_2(\mathbf{x}_0)$ , but outside  $S_1(\mathbf{x}_0)$ , obeys  $\sim \exp(\lambda_2 t)$  as  $t \rightarrow -\infty$ . Recursively, we define a set of nested subspaces,

$$S_1(\mathbf{x}_0) \subset S_2(\mathbf{x}_0) \subset \cdots \subset S_N(\mathbf{x}_0) = \mathbb{R}^N$$

such that if  $\delta \mathbf{u} \in S_n \setminus S_{n+1}$  then  $\lim_{t \rightarrow -\infty} t^{-1} \ln \|\delta \mathbf{u}(t)\| = \lambda_n$ . (In the case degenerate LEs exist, trivial modifications in the above expressions have to be performed.) The backward LVs coincide with the orthonormal vectors obtained as a byproduct of the standard algorithm via Gram-Schmidt orthogonalizations to compute the LEs (Ershov & Potapov 1998).

### 2.2. Forward Lyapunov vectors

The Oseledec theorem can be also formulated in the opposite time limit, defining an operator

$$\Phi_f(t_0) = \lim_{t_2 \rightarrow \infty} [\mathbf{M}^*(t_2, t_0) \mathbf{M}(t_2, t_0)]^{\frac{1}{2(t_2 - t_0)}} \quad (3)$$

such that the LEs are the logarithms of the eigenvalues of  $\Phi_f$  and the eigenvectors form an orthogonal basis, called the forward LVs  $\{\mathbf{f}_n(t_0)\}_{n=1, \dots, N}$ . These vectors are the counterpart of the backward LVs, but now indicating the directions that will grow in the future with exponents  $\lambda_n$ . Like with the backward LVs, the Gram-Schmidt procedure can be used to obtain forward LVs, but now going backwards in time and using the adjoint (e.g., the transposed) Jacobian matrix. As noted by Legras & Vautard (1996), the use of the transposed Jacobian makes the forward LVs to come up with the standard ordering. This means that to obtain the first  $n$  forward LVs we need to integrate only  $n$  perturbations.

For numerical purposes, note that computing forward LVs requires to be able to trace backwards a certain trajectory. This can be done in three different ways:

- (i) Storing a complete trajectory in the computer (ideally in the RAM memory). This is adequate if the system is not invertible, or in time-delayed systems (Pazó & López 2010).
- (ii) Storing periodically the state of the system along the forward integration. This allows to integrate the system backwards, rectifying the trajectory periodically to cancel out the departure from the attractor (now, a repeller) with exponent  $-\lambda_N$ .
- (iii) Integrating backward with a “bit reversible” algorithm. This procedure has no cost of memory but it works only with Hamiltonian systems (Romero-Bastida et al. 2010).

### 2.3. Characteristic (or covariant) Lyapunov vectors

The CLVs  $\{\mathbf{g}_n\}_{n=1, \dots, N}$  form the only truly intrinsic set of Lyapunov vectors, and we will refer to them hereafter simply as the Lyapunov vectors. CLVs are the Floquet eigenvectors in the case of a periodic orbit, they are independent of the definition of the scalar product, and the associated expansion rates are recovered in both, future and past, limits:

$$\lim_{|t| \rightarrow \infty} t^{-1} \ln \|\mathbf{M}(t, t_0) \mathbf{g}_n(t_0)\| = \lambda_n. \quad (4)$$

This property entails covariance with the (forward and backward) dynamics:

$$\mathbf{g}_n(t) \propto \mathbf{M}(t, t_0)\mathbf{g}_n(t_0). \quad (5)$$

We use the symbol of proportionality “ $\propto$ ” instead of “ $=$ ” because the norm and orientation of the vector is arbitrary.

### 3. Computation of CLVs: Wolfe and Samelson formulas

In 2007 Wolfe & Samelson (2007) put forward a method to compute the CLVs from backward and forward LVs, solving a linear set of equations (see below). A remarkable feature of Wolfe and Samelson algorithm is that it contains formulas that should allow to achieve some theoretical progress in questions so far tackled only numerically.

The  $n$ -th (characteristic) LV can be expressed as a linear combination of the first  $n$  backward LVs:

$$\mathbf{g}_n(t) = \sum_{i=1}^n y_i^{(n)}(t)\mathbf{b}_i(t) \quad (6)$$

Wolfe and Samelson found that in addition to the first  $n$  backward LVs, the coefficients  $y_i^{(n)}$  require the computation of only the first  $n - 1$  forward LVs. (This is a great advantage if  $n$  is much smaller than the dimension  $N$  of phase space.) Thus the  $n$ -dimensional vector of coefficients  $\mathbf{y}^{(n)}$  is solution of a equation of the form

$$\mathbf{D}\mathbf{y}^{(n)} = \mathbf{0}, \quad (7)$$

where the  $n \times n$  matrix  $\mathbf{D}$  is equal to  $\mathbf{P}^T\mathbf{P}$ . Hence, as noticed by Kuptsov and Parlitz (Kuptsov & Parlitz 2012), it suffices to solve the equation

$$\mathbf{P}\mathbf{y}^{(n)} = \mathbf{0}. \quad (8)$$

where  $\mathbf{0}$  is the  $(n - 1)$ -dimensional null vector, and  $\mathbf{P}$  is a  $(n - 1) \times n$  matrix with elements

$$P_{ij} = \langle \mathbf{f}_i \cdot \mathbf{b}_j \rangle. \quad (9)$$

$\langle \cdot \rangle$  denotes the scalar product, and the vectors are assumed to be normalized:  $\langle \mathbf{b}_i \cdot \mathbf{b}_j \rangle = \delta_{ij} = \langle \mathbf{f}_i \cdot \mathbf{f}_j \rangle$ . Equation (8) consists of  $n - 1$  equations for  $n$  unknowns. This under-determination is not a problem because (assuming the LE is not degenerate) there exist an obvious indetermination in the modulus and sign of the LV. We impose  $\sum_{i=1}^n [y_i^{(n)}]^2 = 1$ , and hence only the orientation of the vector is not specified.

### 4. The angle between the first and the second Lyapunov vectors

In this work we restrict our study to the angle  $\psi$  between the first and the second LVs:

$$\psi = \angle(\mathbf{g}_1, \mathbf{g}_2). \quad (10)$$

As the signs of  $\mathbf{g}_1$  and  $\mathbf{g}_2$  are arbitrary, we are free to choose them restricting  $\psi$  to the interval  $[0, \frac{\pi}{2}]$ . After some algebra we can obtain from (7) (or (8)) a relation between  $\psi$  and the angles between the two leading backward LVs and the main forward LV,  $\alpha = \angle(\mathbf{b}_1, \mathbf{f}_1)$  and  $\beta = \angle(\mathbf{b}_2, \mathbf{f}_1)$ :

$$\tan \psi = \frac{\cos \alpha}{\cos \beta} \quad (11)$$

In a high-dimensional systems forward and backward LVs are expected to be very seldom parallel. (For instance, the angle  $\phi$  between two random vectors in  $\mathbb{R}^N$

is distributed as  $P(\phi) \propto \sin^{N-2} \phi$ .) Hence, the high dimensionality of phase space suggests to work with the displacements from orthogonality:

$$\delta\alpha = \frac{\pi}{2} - \alpha \quad (12)$$

$$\delta\beta = \frac{\pi}{2} - \beta \quad (13)$$

Equation (11) may be written in these new variables:

$$\tan \psi = \frac{\sin(\delta\alpha)}{\sin(\delta\beta)} \quad (14)$$

In high-dimensional spaces the constraints of  $\mathbf{b}_2$  are so weak that we can legitimately expect  $\delta\alpha$  and  $\delta\beta$  to be very similarly distributed. Notice that as a consequence, since  $\tan(\frac{\pi}{2} - \psi) = 1/\tan \psi$ ,  $\psi$  should be in good approximation distributed symmetrically around  $\frac{\pi}{4}$  (particularly if the system is large). Moreover, as  $\delta\alpha$  and  $\delta\beta$  are expected to be near zero, their quotient should favour values of  $\psi$  close to 0 or  $\frac{\pi}{2}$ . In fact a probability density function (PDF) of  $\psi$  has been recently measured in numerical simulations of a quasi-one-dimensional system of hard disks by Morriss (2012) (see figure 18), finding the aforementioned properties: approximately symmetric around  $\frac{\pi}{4}$  and peaks at 0 and  $\frac{\pi}{2}$ . These features are also observed in our simulations (see below) in one-dimensional systems with extensive chaos. Note though that eq. (14) is valid in any dimension.

A much finer analysis is needed to understand the statistics of  $\psi$ , particularly close to the tangency of leading Oseledec subspaces  $\psi \rightarrow 0$ . This is studied in detail in section 6.

## 5. Numerical models

In this section we introduce the two systems we have numerically investigated, and present our first numerical results. The first one is a coupled-map lattice (CML), and the second one is a minimal stochastic model of the LVs. Both systems were previously studied by Szendro et al. (2007) and Pazó et al. (2008), respectively, and are good test-bed systems with generic properties of spatio-temporal chaotic system.

### 5.1. Coupled-map lattice

Our one-dimensional CML reads:

$$u_j(t+1) = \epsilon \{f[u_{j+1}(t)] + f[u_{j-1}(t)]\} + (1-2\epsilon)f[u_j(t)], \quad (15)$$

where the index  $j$  runs from 1 to  $L$  (the system size), with periodic boundary conditions:  $u_0(t) = u_L(t)$  and  $u_{L+1}(t) = u_1(t)$ . Like in (Szendro et al. 2007), the coupling parameter is chosen to be  $\epsilon = 0.1$ , and  $f$  is the logistic map  $f(y) = 4y(1-y)$ . With these parameters the system is hyperchaotic with  $\lambda_n > 0$  for  $n/L < 0.795$ .

Our numerical simulations confirm that as anticipated in the previous section the PDF of  $\psi$  is roughly symmetric around  $\frac{\pi}{4}$ , see Fig. 1.  $P(\psi)$  is peaked at 0 and  $\frac{\pi}{2}$ . However the distribution is not perfectly symmetric, and this unbalance becomes more significant as the system size increases. Which is the asymptotic behaviour of this unbalance as the system size increases will be a subject for future research.

Concerning the spatial organization of the CLVs, as they are known to be highly localized (Pikovsky & Politi 1998, Szendro et al. 2007), a probability of  $\psi$  peaked at 0, is consistent with an intermittent coincidence of the localization sites of the first

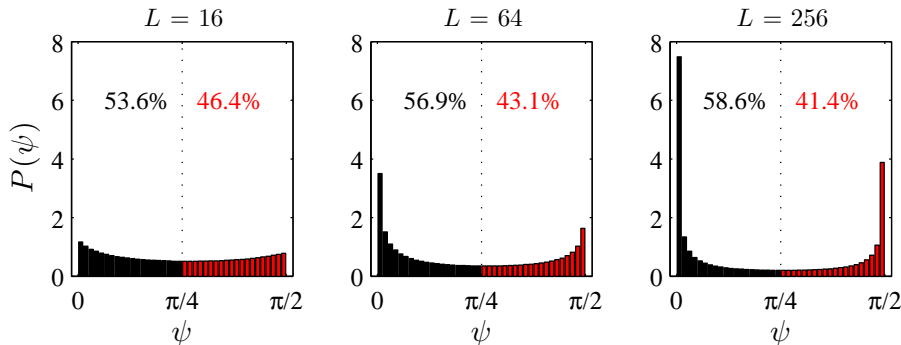


**Figure 1.** Distribution of  $\psi$  for the CML (15) and three different system sizes. The percentages refer to cumulative probabilities  $\int_0^{\pi/4} P(\psi)d\psi$  and  $\int_{\pi/4}^{\pi/2} P(\psi)d\psi$ .

and second LVs. This is observed in this CML (Szendro et al. 2007) and other systems with spatio-temporal chaos (Pazó et al. 2008, Romero-Bastida et al. 2010, Herrera et al. 2011), and in time-delayed systems (Pazó & López 2010).

### 5.2. Minimal stochastic model

In two seminal works Pikovsky & Kurths (1994) and Pikovsky & Politi (1998) proposed the multiplicative stochastic linear equation

$$\partial_t w(x, t) = \zeta(x, t)w(x, t) + \partial_{xx}w(x, t) \quad (16)$$

as a minimal model for the tangent space dynamic of spatio-temporal chaos.  $w$  represents the infinitesimal perturbation and  $\zeta$  is a stochastic forcing that mimics the chaotic forcing of the field.  $\zeta(x, t)$  is in general short-range correlated, and hence it can be simply assumed to be zero-mean white noise with  $\langle \zeta(x, t) \zeta(x', t') \rangle = 2\sigma \delta(x - x') \delta(t - t')$ , as this assumption does not affect the long-scale and long-time scaling properties of  $w$ . Under a Hopf-Cole transformation,  $h(x, t) = \ln |w(x, t)|$ , equation (16) becomes the KPZ equation (Kardar et al. 1986)

$$\partial_t h(x, t) = \zeta(x, t) + [\partial_x h(x, t)]^2 + \partial_{xx}h(x, t), \quad (17)$$

which is a paradigmatic equation in the field of growing rough surfaces (Barabási & Stanley 1995). Under a Hopf-Cole transformation, the first LV falls into the universality class of the KPZ equation. And thus, the large-scale spatial and temporal scaling properties of the LV are common to very different system types (Pikovsky & Politi 1998, Pazó & López 2010), excluding Hamiltonian lattices (Pikovsky & Politi 2001) and disordered systems (Szendro et al. 2008).

In dynamical systems generic infinitesimal perturbations tend to align with the first LV, whereas a measure zero set of perturbations may approach saddle-solutions of the linear tangent model, which are precisely the subleading LVs (i.e., corresponding to LEs smaller than the largest one). In our previous work (Pazó et al. 2008) we resorted to (16) as a minimal equation for the sub-leading LVs. We assumed sub-leading LVs correspond to saddle solutions of (16) for a given realization of the noise. In fact we observed that sub-leading LVs in systems with spatio-temporal chaos and the saddle solutions of (16) display the same scaling and statistical properties. This similarity is realized after taking the Hopf-Cole transformation of the LVs (Pazó et al. 2008).

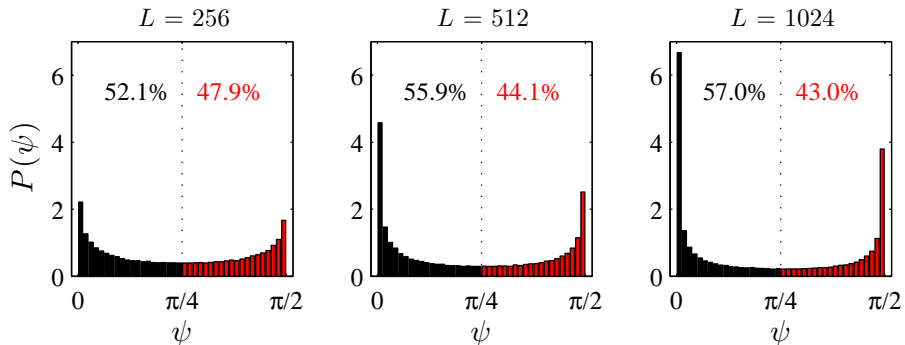


**Figure 2.** Distribution of  $\psi$  for the minimal stochastic model (16).

In our simulations of the minimal stochastic model we have selected  $\sigma = 0.5$ , like in (Pazó et al. 2008), for the variance of the noise. Integration of several copies of (16) under periodic orthonormalizations produces a set of vectors with the same spatio-temporal structure than backward LVs (Pazó et al. 2008) in a typical spatially extended chaotic system. The equation for forward LVs is exactly the same as (16) (because the operator in the right-hand side is self-adjoint). This means that a meaningful  $n$ -th CLV can be computed from the sets of  $n$  backward and  $n - 1$  forward LVs obtained with the standard method (Benettin et al. 1980) integrating eq. (16) with independent white noises  $\zeta_b$  and  $\zeta_f$ , respectively. Note that the obtained CLV at time  $t_0$  is indeed a saddle solution of (16) for a particular realization of the noise:  $\zeta = \zeta_b$  (for  $t \leq t_0$ ) and  $\zeta = \zeta_f$  (for  $t > t_0$ ). The advantage of this procedure is that we can achieve good statistics for the CLVs without the need for time-reversing the trajectory (i.e. the noise). The result of our numerical simulations is shown in figure 2 and, as expected, exhibits the same qualitative features observe in figure 1 for the CML.

## 6. PDF of $\psi$ near the tangency ( $\psi = 0$ )

To analyse the asymptotics of  $P(\psi)$  for  $\psi \rightarrow 0$ , it is useful to use the log-transformed variable

$$\psi_l \equiv \ln \psi, \quad (18)$$

denoted by the subscript  $l$ , likewise for  $\delta\alpha_l$  and  $\delta\beta_l$ . Let  $Q$  be the PDF of  $\psi_l$ , with the trivial relation

$$Q(\psi_l) = P(\psi)\psi \quad (19)$$

The occurrence of tangencies ( $\psi = 0$ ) corresponds to a nonvanishing probability at zero, i.e.  $\lim_{\psi \rightarrow 0} P(\psi) = k > 0$ . Making a transformation into variable  $\psi_l$  this translates into an exponential dependence:

$$\lim_{\psi_l \rightarrow -\infty} Q(\psi_l) = k e^{\psi_l} \quad (20)$$

This asymptotic dependence in logscale is observed in figure 3(a) for the CML, and we conclude that  $P(\psi = 0) = k(L) > 0$  with  $k$  monotonically increasing with  $L$ . Remarkably, despite the similarities observed between the CML and the minimal

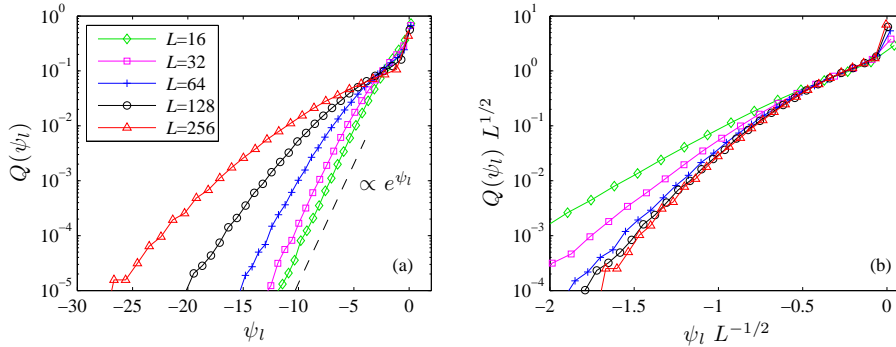


**Figure 3.** (a) PDF  $Q$  of  $\psi_l \equiv \ln \psi$  for the CML, eq. (15). For small systems the true asymptotic law  $Q(\psi_l \rightarrow -\infty) \propto e^{\psi_l}$  can be detected. (b) Data collapse via the scaling relation (21). The region of data collapse progressively enlarges as the system size grows.

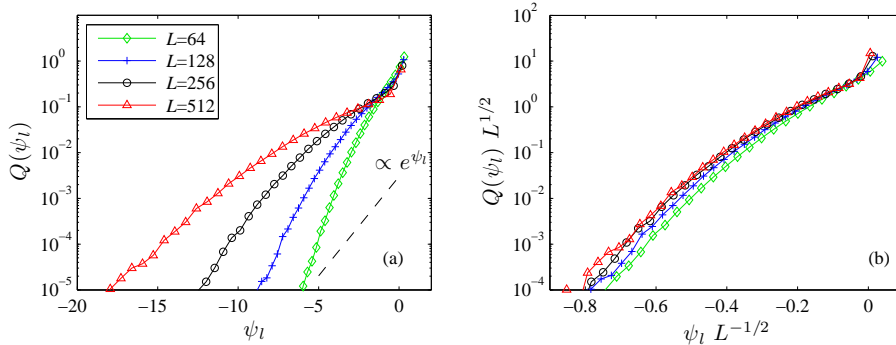


**Figure 4.** (a) PDF of  $\psi_l$  for the minimal stochastic model (16) and different system sizes. The decay as  $\psi_l \rightarrow -\infty$  is faster than  $e^{\psi_l}$ , and consistent with  $P(\psi = 0) = 0$ . (b) Data collapse via the scaling relation (21). The region of data collapse progressively enlarges as the system size grows.

stochastic model, the latter behaves differently: in figure 4(a) we may see that the PDF of  $\psi_l$  decays faster than the exponential for the minimal stochastic model. In fact we may prove that  $P(\psi = 0) = 0$ : in the minimal stochastic model the first LV (either backward or forward because obey the same equation) has the same sign in all the domain (Pikovsky & Politi 1998, Pazó et al. 2008), and in consequence  $\cos \alpha = \langle \mathbf{f}_1 \cdot \mathbf{b}_1 \rangle$  in eq. (11) cannot vanish.

The PDF of  $\psi$  for the CML and the minimal stochastic model in figures 1 and 2 look similar, but figures 3(a) and 4(a) evidence that the behaviour of the PDF for  $\psi \rightarrow 0$  is very different in each model. We have found nonetheless that if  $\psi$  is small but not extremely small, there exist large enough values of  $L$  such that the PDF  $Q$  satisfies the scaling relation:

$$Q(\psi_l) = L^{-1/2} f(\psi_l L^{-1/2}) \quad (21)$$

We may see in figures 3(b) and 4(b) that there is a very good data collapse after scaling  $\psi_l$  by  $L^{-1/2}$ . Only when  $\psi_l L^{-1/2}$  becomes smaller than a certain value  $c(L)$  the peculiarities of each model show up. Note that as  $c(L)$  decreases with  $L$  the



departure from the scaling law (21) is not detectable for large systems. Remarkably the departure from (21) due to the finiteness of  $L$  occurs upwards for the CML, and downwards for the minimal stochastic model, reflecting their intrinsically different values of  $P(\psi = 0)$ .

We emphasize that it is crucial to distinguish between the limit  $\psi \rightarrow 0$  at large (but finite)  $L$  and the limit  $L \rightarrow \infty$  at small (but nonzero)  $\psi$ . In the former case each model exhibits its peculiarities and the stochastic model does not capture the true behaviour for chaotic systems, which we expect to be generally like the CML. In fact, tangencies are believed to occur between “physical” modes (Yang et al. 2009). However in the limit  $L \rightarrow \infty$  the stochastic model captures the statistics of  $\psi_l$  in the CML and presumably other chaotic systems. Moreover we can justify the form of the scaling relation in eq. (21) by virtue of some theoretical arguments that we develop in the next section.

## 7. Theoretical analysis

Close to tangency we can approximate  $\tan \psi$  by  $\psi$ . In addition we recall that  $\delta\alpha$  and  $\delta\beta$  can be expected to be close to zero most of the time (as observed in the simulations, and not shown). Hence in good approximation:

$$\psi = \frac{\delta\alpha}{\delta\beta} \quad (22)$$

In the log-transformed variables this relation becomes a subtraction

$$\psi_l = \delta\alpha_l - \delta\beta_l \quad (23)$$

Let  $G(\delta\alpha_l, \delta\beta_l)$  to denote the joint PDF of  $\delta\alpha_l$  and  $\delta\beta_l$ . An auxiliary variable  $\rho = \delta\alpha_l + \delta\beta_l$  allows to relate  $Q$  and  $G$  through the integral:

$$Q(\psi_l) = \frac{1}{2} \int_{-\infty}^{\psi_l + 2 \ln \frac{\pi}{2}} G\left(\frac{\rho + \psi_l}{2}, \frac{\rho - \psi_l}{2}\right) d\rho \quad (24)$$

where we are assuming  $\psi_l < 0$ .  $\delta\alpha$  and  $\delta\beta$  are not completely independent variables (e.g., in the seldom event that one of them equals  $\frac{\pi}{2}$  the other one becomes 0). However when both of them are close to zero—which occurs most of the time—we can expect them to be basically independent and the PDF factorizes:  $G(\delta\alpha_l, \delta\beta_l) \approx A(\delta\alpha_l)B(\delta\beta_l)$ . We get then

$$Q(\psi_l) \approx \frac{1}{2} \int_{-\infty}^{\psi_l + 2 \ln \frac{\pi}{2}} A\left(\frac{\rho + \psi_l}{2}\right) B\left(\frac{\rho - \psi_l}{2}\right) d\rho. \quad (25)$$

We are interested in the  $\psi_l \rightarrow -\infty$  limit of this formula.

It is convenient to make a change of variable:  $x = \frac{\rho - \psi_l}{2}$ , such that

$$Q(\psi_l) \approx \int_{-\infty}^{\ln \frac{\pi}{2}} A(x + \psi_l) B(x) dx. \quad (26)$$

This equation suggests that the asymptotics of the PDF of  $\psi$  as  $\psi \rightarrow 0$  ( $\psi_l \rightarrow -\infty$ ) is highly influenced (if not determined) by  $A$ . So we focus our interest in the next section on the distribution of  $\delta\alpha$ .

7.1. PDF of  $\delta\alpha$ 

Recall  $\alpha$  is the angle between the first backward LV and the first forward LV. In a previous work (Pazó et al. 2008) we found that both vectors are well modeled by the multiplicative stochastic equation (16). As we reasoned in Sec. 5.2 the stochastic equation can be used to get the statistics of characteristic LVs. We have to integrate the fields  $b_1(x, t)$  and  $f_1(x, t)$ , and the angle  $\alpha$  between them is obtained from a continuous version of the Euclidean scalar product (in practice the fields are discretized so we compute the usual Euclidean scalar product):

$$\cos \alpha = \frac{\langle b_1 \cdot f_1 \rangle}{\langle b_1 \cdot b_1 \rangle^{1/2} \langle f_1 \cdot f_1 \rangle^{1/2}} = \frac{\int_0^L b_1 f_1 dx}{\left( \int_0^L b_1^2 dx \right)^{1/2} \left( \int_0^L f_1^2 dx \right)^{1/2}}. \quad (27)$$

A logarithmic transformation allows to define the associated surface for the first backward LV,  $h_b(x, t) = \ln b_1(x, t)$ , and the first forward LV,  $h_f(x, t) = \ln f_1(x, t)$ . Under this transformation  $h_b$  and  $h_f$  are governed by the KPZ equation (17). We further decompose  $h_b$  into the spatial average and the fluctuating part  $h_b(x) = \bar{h}_b + B_b(x)$  (and likewise for  $h_f$ ).  $\bar{h}_b$  is fixed by the norm of the vector and therefore the result must be independent of the norm used. Some algebra yields the expression:

$$\cos \alpha = \frac{\int_0^L e^{B_b(x)+B_f(x)} dx}{\left( \int_0^L e^{2B_b(x)} dx \right)^{1/2} \left( \int_0^L e^{2B_f(x)} dx \right)^{1/2}} \quad (28)$$

$B_b$  and  $B_f$  are independent profiles *with zero mean*. In particular,  $B_b$  and  $B_f$  are at long scales indistinguishable from a Brownian path in one dimension, see (Pikovsky & Politi 1998), like solutions of the KPZ equation. This kind of integrals in (28) have been subject of some mathematical interest (Matsumoto & Yor 2005) but unfortunately the theory is not mature yet as to provide results that one can readily use here, specially if different integrals are correlated.

Equation (26) suggests small  $\psi_l$  is controlled by the PDF asymptotic behaviour of  $A(\delta\alpha_l \rightarrow -\infty)$ , so we make the approximation  $\cos \alpha = \sin(\delta\alpha) \approx \delta\alpha$ , in the left hand side of (28). Next, taking the logarithms we obtain:

$$\delta\alpha_l \simeq \ln \left( \int_0^L e^{B_b(x)+B_f(x)} dx \right) - \frac{1}{2} \ln \left( \int_0^L e^{2B_b(x)} dx \right) - \frac{1}{2} \ln \left( \int_0^L e^{2B_f(x)} dx \right) \quad (29)$$

## 7.2. Scaling with the system size

From eq. (29), and recalling  $B_b$  and  $B_f$  are like two independent Brownian paths, we can expect a scaling with the system size of the form  $\delta\alpha_l \sim \sqrt{L}$ . This is expected to translate to  $\psi_l$  in the form of the scaling relation in eq. (21). We may also conjecture that in two spatial dimensions the scaling factor in (21) should be  $L^{-\alpha_{2dKPZ}}$ ,  $\alpha_{2dKPZ} \approx 0.387$  (Forrest & Tang 1990), instead of  $L^{-1/2}$ .

We can also conjecture that in the minimal stochastic model the PDF  $P(\psi)$  vanishes not only at  $\psi = 0$  but in an interval below a certain value  $\psi^c$ ; i.e.  $P(0 \leq \psi < \psi^c) = 0$ . Note that in the most unfavourable situation, if  $B_b + B_f = 0$ , the numerator of (28) equals  $L$ . And the denominator is maximal if  $B_b$  (and  $B_f$ ) has a triangular shape. In this case the denominator grows exponentially with  $L$ , and in turn  $\delta\alpha_l$  is likely to have the infimum  $\delta\alpha_l^c$  decreasing exponentially with  $L$ . Hence  $\delta\alpha_l^c \sim -L$ , and looking at eq. (26) we presume a similar dependence for the bound for  $\psi_l^c \sim -L$ .

## 8. Discussion and conclusions

In the first part of this paper we have seen that Wolfe and Samelson formulas allow to foresee the general form of  $P(\psi)$ , which should be general in high-dimensional systems and irrespective of the dissipative or conservative character of the dynamics and of the spatial dimensionality. In the second part of the paper, we obtained a scaling law resorting to a minimal stochastic model of the LVs for spatio-temporal chaos.

The reason for the general validity of our scaling law (21) is that although specific system-dependent correlations between forward and backward LVs exist due to the deterministic nature of the dynamics, these correlations are not expected to span much beyond the Lyapunov time  $\lambda_1^{-1}$ . In contrast, in typical systems with spatio-temporal chaos (Pikovsky & Politi 1998), see also (Pikovsky & Politi 2001), the backward (forward) LVs depend on the past (future) within large temporal range of order  $L^z$  (with  $z = \frac{3}{2}$  for the KPZ universality class in one spatial dimension).

Our scaling (21) should be generally observed in spatially extended systems, but the exact asymptotics of the PDF at extremely small  $\psi$  is specific for each system, which would be far beyond numerical capabilities already for moderately large systems. Our results should be taken into account in numerical experiments with CLVs because if  $L$  is large we may not detect what is peculiar for each model, but just generic model-independent features.

So far the tools borrowed from surface roughening formalism have been probably the most useful ones in providing theoretical results for the Lyapunov vectors in spatio-temporal chaos. This work underpins the might of this approach.

## Acknowledgments

DP acknowledges support by Ministerio de Economía y Competitividad (Spain) through the Ramón y Cajal programme. Financial support from the Ministerio de Ciencia e Innovación (Spain) under projects No. FIS2009-12964-C05-05 and No. CGL2010-21869 is acknowledged.

## References

- Barabási A L & Stanley H E 1995 *Fractal Concepts in Surface Growth* Cambridge University Press Cambridge.
- Benettin G, Galgani L, Giorgilli A & Strelcyn J M 1980 *Meccanica* **15**, 9–20.
- Bosetti H & Posch H A 2010 *Chem. Phys.* **375**, 296–308.
- Cross M C & Hohenberg P C 1993 *Rev. Mod. Phys.* **65**, 851–1112.
- Eckmann J P & Ruelle D 1985 *Rev. Mod. Phys.* **57**, 617–656.
- Ershov S V & Potapov A B 1998 *Physica D* **118**, 167–198.
- Forrest B M & Tang L H 1990 *Phys. Rev. Lett.* **64**, 1405–1408.
- Ginelli F, Poggi P, Turchi A, Chaté H, Livi R & Politi A 2007 *Phys. Rev. Lett.* **99**, 130601.
- Herrera S, Pazó D, Fernández J & Rodríguez M A 2011 *Tellus A* **63**, 978–990.
- Kalnay E 2002 *Atmospheric Modeling, Data Assimilation and Predictability* Cambridge University Press Cambridge.
- Kardar M, Parisi G & Zhang Y C 1986 *Phys. Rev. Lett.* **56**, 889–892.
- Kuptsov P V & Parlitz U 2010 *Phys. Rev. E* **81**, 036214.
- Kuptsov P V & Parlitz U 2012 *J. Nonlinear Sci.* **22**, 727–762.
- Legras B & Vautard R 1996 in T Palmer, ed., ‘Proc. Seminar on Predictability Vol. I’ ECMWF Seminar ECMWF Reading, UK pp. 135–146.
- Matsumoto H & Yor M 2005 *Probab. Surv.* **2**, 312–347.
- Morriss G P 2012 *Phys. Rev. E* **85**, 056219.
- Morriss G P & Truant D P 2013 *J. Phys. A: Math. Gen.* **46**, 254010.

- Ng G H C, Mclaughlin D, Entekhabi D & Ahanin A 2011 *Tellus A* **63**, 958–977.
- Oseledec V I 1968 *Trans. Moscow Math. Soc.* **19**, 197–221.
- Ott E 1993 *Chaos in Dynamical Systems* Cambridge University Press Cambridge.
- Pazó D & López J M 2010 *Phys. Rev. E* **82**, 056201.
- Pazó D, Rodríguez M A & López J M 2010 *Tellus A* **62**, 10–23.
- Pazó D, Szendro I G, López J M & Rodríguez M A 2008 *Phys. Rev. E* **78**, 016209.
- Pikovsky A & Politi A 1998 *Nonlinearity* **11**, 1049–1062.
- Pikovsky A & Politi A 2001 *Phys. Rev. E* **63**, 036207.
- Pikovsky A S & Kurths J 1994 *Phys. Rev. E* **49**, 898–901.
- Romero-Bastida M, Pazó D, López J M & Rodríguez M A 2010 *Phys. Rev. E* **82**, 036205.
- Ruelle D 1979 *Commun. Math. Phys.* **87**, 287–302.
- Szendro I G, López J M & Rodríguez M A 2008 *Phys. Rev. E* **78**, 036202.
- Szendro I G, Pazó D, Rodríguez M A & López J M 2007 *Phys. Rev. E* **76**, 025202(R).
- Taniguchi T & Morriss G P 2005 *Phys. Rev. Lett.* **94**, 154101.
- Trevisan A & Pancotti F 1998 *J. Atmos. Sci.* **55**, 390–398.
- Wolfe C L & Samelson R M 2007 *Tellus A* **59**, 355–366.
- Yang H L & Radons G 2008 *Phys. Rev. Lett.* **100**, 024101.
- Yang H L, Takeuchi K A, Ginelli F, Chaté H & Radons G 2009 *Phys. Rev. Lett.* **102**, 074102.